

# Lamellar separation during the deformation of high-density polyethylene

J. PETERMANN\*, J. M. SCHULTZ

*Department of Chemical Engineering University of Delaware, Newark, Delaware 19711, USA*

Upon tensile straining at low deformation rates ( $\dot{\epsilon} = 2 \times 10^{-5} \text{ sec}^{-1}$ ), spherulitic linear polyethylene behaves reversibly for extensions up to 40%. In stress relaxation experiments on unloaded specimens the stress increases with time. Samples kept under constant strain ( $\epsilon = 40\%$ ) over four months show macroscopic cracking. Microstructural investigation was performed using low- and wide-angle X-ray diffraction and transmission electron microscopy. These investigations reveal a very inhomogeneous deformation within those lamellar stacks for which the crystalline lamellae lie normal to the tensile axis. The deformation in that case is similar to what has been observed for "elastic hard fibres". A two-mechanism model to explain the macroscopic observation on the basis of the microscopic observations is developed.

## 1. Introduction

Deformation processes in semicrystalline polymers are strongly influenced by the orientation of the crystalline lamellae, as well as the amorphous layers, with respect to the tensile direction [1-3]. For highly oriented "elastic hard fibres", where the lamellae are normal to the tensile direction [4, 5], the yield stress is much higher than in spherulitic material with a radial orientation of the lamellae. Furthermore, "elastic hard fibres" exhibit a reversible extension over a range of 100% without necking. Upon straining such material, the lamellae become separated, except where they are bound together by small fibrils. The surface energy created during the separation has been shown to be the retractive force resulting in the reversibility of the deformation [6].

In spherulitic material the reversible part of the stress-strain curve (for polyethylene  $\leq 20\%$ ), has been attributed to a straining of the amorphous content [7]. Higher elongation results in chain tilting, crystallographic slip, twinning and chain unfolding [8-14]. Furthermore, interlamellar and interspherulitic slip are deformation modes for polymeric crystalline aggregates also [11, 15].

It is the purpose of this work to investigate whether, and perhaps to what level, lamellar separation (of the type observed in the "elastic hard fibres") takes part in the deformation processes in spherulites, and to consider mechanical consequences of this deformation mode.

## 2. Experimental

The material used was unfractionated Marlex 6009, a linear polyethylene supplied by the Phillips Chemical Company. The polymer was pressed into 2 mm thick plates, melted at 170°C, quenched into water and subsequently annealed at 125°C for two hours. Samples with a 2 mm  $\times$  25 mm cross-section and a gauge length of 50 mm were machined from the plates.

Mechanical testing was carried out in an Instron tester. The deformation was done at 22°C, with a strain rate of  $2 \times 10^{-5} \text{ sec}^{-1}$ . One test was, however, performed at 70°C. All textual reference will be to 22°C deformation, unless specifically indicated otherwise.

For X-ray investigations, the strained samples were clamped into a picture frame device, in order to maintain a constant elongation. Small-angle

\*Current address: Werkstoffphysik, Bau 2, Universität des Saarlandes, 66 Saarbrücken, West Germany

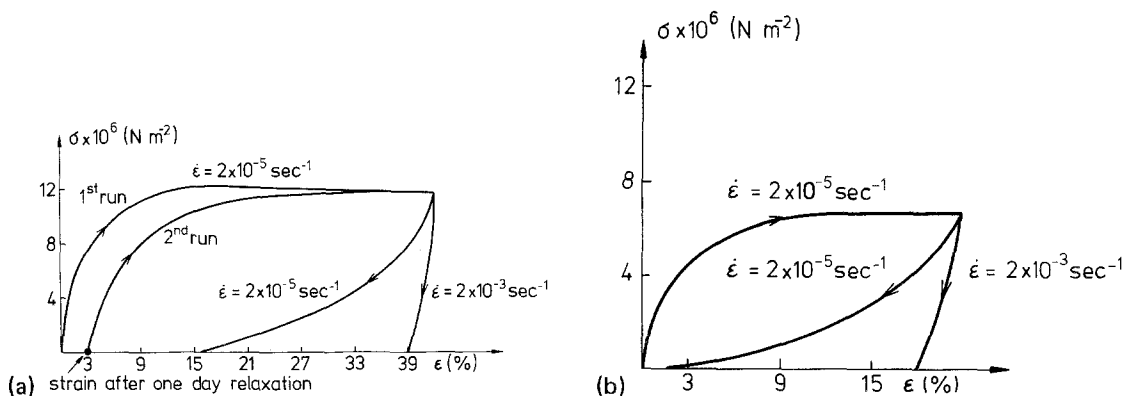


Figure 1 (a) The nominal stress–strain curve for straining and destraining a spherulitic polyethylene sample at 22° C. The strain rate is  $2 \times 10^{-5} \text{ sec}^{-1}$  for straining,  $2 \times 10^{-5} \text{ sec}^{-1}$  and  $2 \times 10^{-3} \text{ sec}^{-1}$  for destraining. The second run was made after one day of strain recovery. (b) The nominal stress–strain curve for straining and destraining a spherulitic polyethylene sample at 70° C. Strain rates are the same as in Fig. 1a.

X-ray scattering (SAXS) was performed using a Kratky camera, with  $\text{FeK}\alpha$  radiation. Some SAXS data was obtained using a Franks camera, in order to observe orientation effects. A pinhole camera was used for wide-angle X-ray scattering (WAXS).

Melt-cast films, composed of a twisted lamellar microstructure, were used for transmission electron microscopy. The electron microscope was a JEM 200 A, operated in phase contrast [16] at 100 kV.

### 3. Results

On straining samples at room temperature and 70° C, nominal stress–strain curves show two regions: an initial parabolic-appearing increase of the stress, followed by a plateau region. This is seen in Fig. 1. With the low strain rates ( $2 \times 10^{-5} \text{ sec}$  used here, uniform extension over the whole gauge length is observed up to a strain of 40%. Higher strain results in localized deformation of

up to 100%. Before macroscopic necking occurs, the draw ratio,  $\lambda = l/l_0$ , of the samples was taken from marks printed on the samples prior to drawing. Higher strain rates result in a smaller draw ratio of the pre-necked zone. The reversibility of the extension depends on the strain rate and time of unloading [Fig. 1a]. After 24 h, strain recovery is completed to within 3% of the initial length in a sample which had been strained 40%. Fig. 2 shows the pinhole X-ray pattern of the samples prior to straining, in the strained state and after 24 h strain recovery. It can be seen that an orientation change is nearly recoverable after unloading.

The pinhole SAXS patterns change from a circular diffraction ring into an elliptical shape. In Fig. 3 the Kratky scans of undeformed and deformed samples are shown. The long period of the undeformed sample is 260 Å. No precise long period parallel to the drawing directional of the

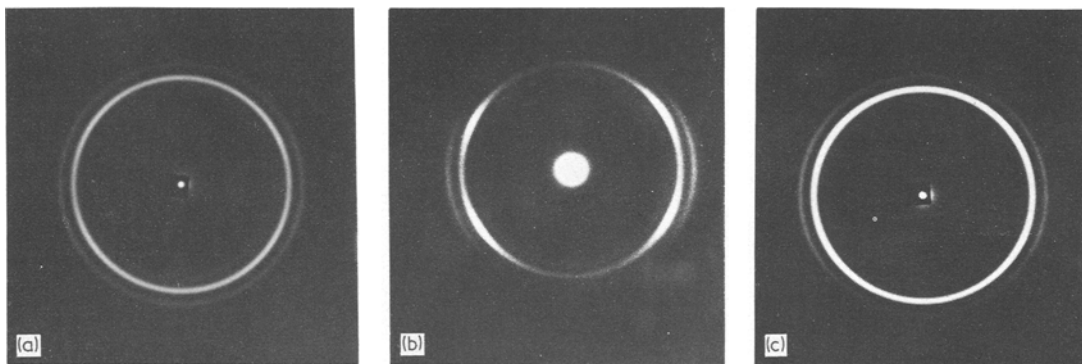


Figure 2 (a) WAXS pinhole patterns of a non-deformed sample. (b) WAXS pinhole patterns of a sample strained 40% at 22° C. (c) WAXS pinhole patterns of the same sample after one day strain recovery.

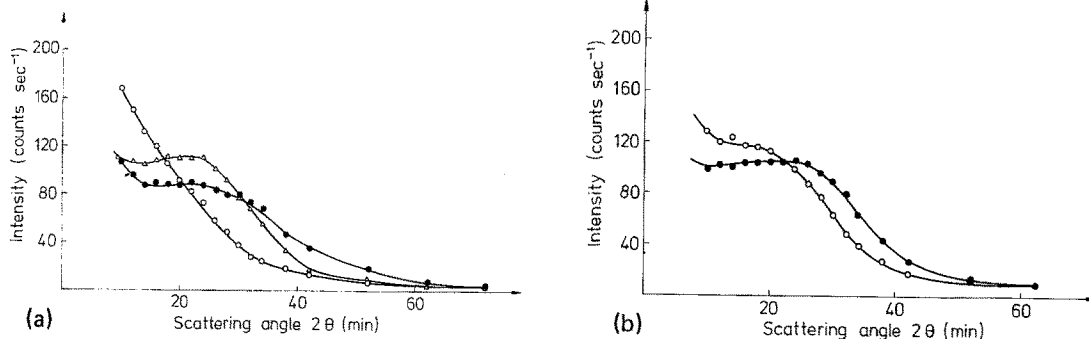


Figure 3 (a) Slit-smear SAXS of an undeformed sample ( $\Delta$ ), and a 40% strained sample, slit perpendicular ( $\circ$ ) and parallel ( $\bullet$ ) to the strain direction. (b) Slit-smear SAXS of a 40% deformed sample, subsequently strain recovered for one day, slit perpendicular, ( $\circ$ ) and parallel ( $\bullet$ ) to the strain direction.

deformed sample could be detected and the perpendicular long period decreases to 210 Å. After strain recovery, the long periods are 275 Å and 220 Å, respectively.

When deforming a thin film with twisted lamellar structure in the straining device of the electron microscope, a rather irregular separation of the lamellae located perpendicular to the drawing direction is observed (Fig. 4). Upon unloading, the gaps between the lamellae contract.

#### 4. Discussion

The shape of the stress-strain curves (Fig. 1) is similar to that of an "elastic hard fibre", with the yield stress being smaller by a factor of seven [6] and the high reversibility being obtained only with low deformation rates. The temperature dependence of the yield stress excludes an entropy elasticity as well. Small-angle X-ray (SAXS) results

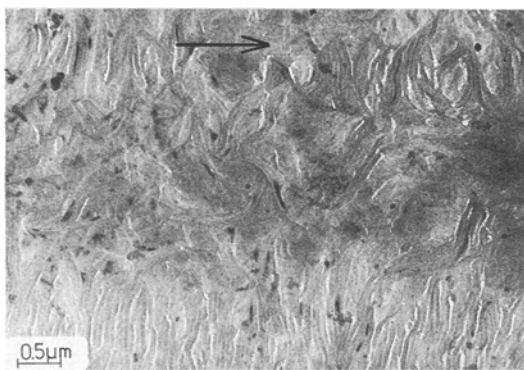


Figure 4 Transmission electron micrograph of a deformed polyethylene film with twisted lamellae ( $\epsilon$  about 40%). The white lines are gaps between crystalline lamellae, the striations between the white lines are fibrils interconnecting the lamellae. The arrow indicates the chain direction.

(Fig. 3) and the electron micrograph (Fig. 4) show that lamellar separation during straining occurs and that the separation is, to a great extent, reversible. The SAXS curves for lamellae perpendicular to the draw direction has the form of a void scattering. Such a pattern would be qualitatively predicted for irregular and uneven lamellar separations, as expected from a non-uniform deformation of amorphous zones and the creation of effective void (or low-density) zones between crystallites. In contrast to the elastic hard fibres, where the molecular orientation within the sample does not change during straining, a change occurs in spherulitic material and has been attributed by many authors to different deformation modes. Upon unloading, a retractive force deforms the crystallites into their initial orientation (Fig. 3).

In order to understand the macroscopic and microscopic effects reported, the deformation model illustrated in Fig. 5 is proposed. Above an extension where only amorphous parts are strained, lamellae which lie perpendicular to the tensile direction become separated. With only a few percent of the lamellae having this orientation (region A in Fig. 5), the other areas (region B) of the spherulite have to deform by other deformation modes, giving rise to the change in the WAXS pattern. While the other deformation modes (slip, chain kinking, etc.) are mainly plastic, the separation process is elastic for the same reason as in elastic hard fibres. Furthermore, the stress to separate two lamellae is higher than the stress for shearing lamellae. Therefore local stress concentrations will build up. When unloading the sample to zero stress, the retractive force in region A, resulting from a surface elasticity, will not

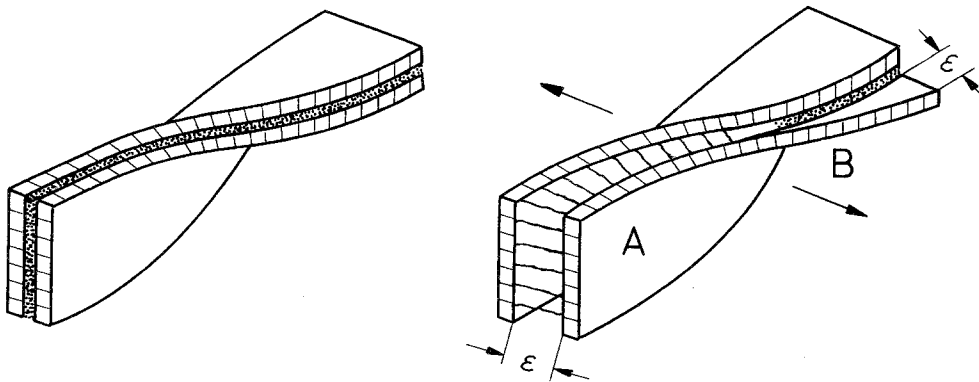


Figure 5 Sketch of non-deformed and deformed ( $\epsilon$ ) twisted lamellae. In region A, the deformation is performed by separating the lamellae, in region B by interlamellar slip. The interlamellar slip can be replaced by any (or all) of the other deformation modes mentioned in the text.

change greatly with time as long as the lamellae are separated. In region B, the deformed structure can recover, meaning that it becomes less resistant to the retractive stress. The recovery is due to a thermally-activated rearrangement of molecules or lattice defects into a state of lower energy. Macroscopically, the sample has then a tendency to shrink, or, when keeping the strain constant, a macroscopic stress builds up. In Fig. 6, the increase of stress with time is shown. This kind of mechanical behaviour is known as creep recovery, or the elastic after-effect, and has been previously attributed to inhomogeneous stress distributions [17]. In our model, the internal energy of the sample can be lowered by lowering the internal surface area. This will be the case if

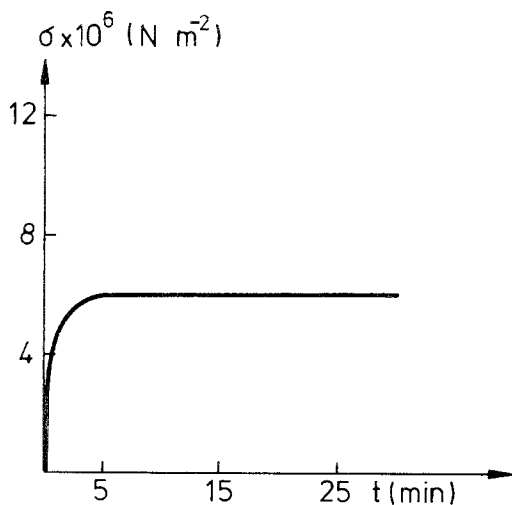


Figure 6 The increase of stress with time for a sample which had been deformed 40% and unloaded with a strain rate of  $\dot{\epsilon} = 2 \times 10^{-3} \text{ s}^{-1}$  to zero stress.

many small gaps close up and form large cracks of localized deformed areas. Fig. 7 shows a strained sample kept under constant strain over a period of eight weeks. Stress cracking and highly deformed areas can be seen.

## 5. Conclusions

(1) Strain and orientation recover, but slowly, for deformations up to 40%.

(2) SAXS and electron microscopy indicate irregular separation for crystallites oriented perpendicular to the stress direction.

(3) Unloaded but constrained material shows a very large building of stress with time.

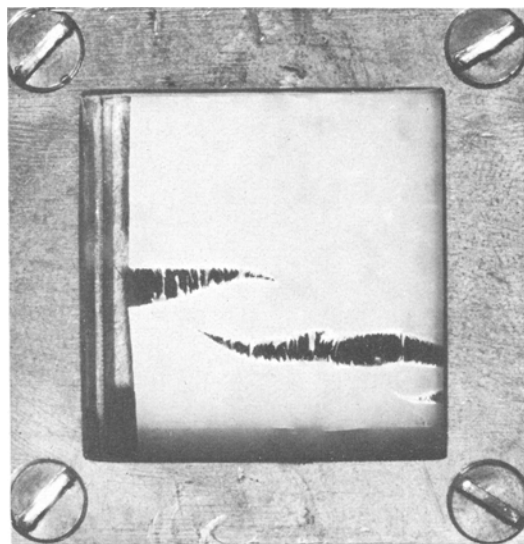


Figure 7 Deformed sample ( $\epsilon = 40\%$ ) kept under constant strain for a period of four months. Macroscopic cracks can be seen.

(4) The mechanical behaviour of the material can be explained on a two-mechanism model. In this model, the lamellae normal to the stress direction deform by extension of chains in the amorphous regions. Crystallites oriented at smaller angles to the stress deform by shear process and can creep in order to reduce the strain energy density.

(5) On unloading, the response is controlled by the creep recovery of those crystalline elements which lie at smaller angles to the deformation direction.

## References

1. S. NAMURA, M. MATSUO and H. KAWAI, *J. Polymer Sci. A-2* **10** (1972) 2489.
2. K. SASAGURI, R. YAMADA and R. S. STEIN, *J. Appl. Phys.* **35** (1964) 3188.
3. T. T. WANG, *J. Polymer Sci., Polym. Phys. Ed.* **2** (1964) 145.
4. E. S. CLARK, "Structure and Properties of Polymer Films," edited by R. W. Lenz and R. S. Stein (Plenum Press, New York, 1974).
5. B. S. SPRAGUE, *J. Macromol. Sci. -Phys.*, **B-8** (1973) 157.
6. M. MILES, J. PETERMANN and H. GLEITER, *ibid* **B-12** (1976) 549.
7. W. E. KAUFMAN and J. M. SCHULTZ, *J. Mater. Sci.* **8** (1973) 41.
8. I. L. HAY and A. KELLER, *Kolloid-Z. u. Z. Polymere*, **204** (1965) 43.
9. A. KELLER and D. P. POPE, *J. Mater. Sci.* **6** (1971) 453.
10. D. A. ZAUKELIES, *J. App. Phys.*, **33** (1962) 2797.
11. A. PETERLIN and G. MEINEL, *Makromol. Chem.* **142** (1971) 227.
12. M. YAMADA, K. MIYASAKA and K. ISHIKAWA, *J. Polymer Sci. A-2* **9** (1971) 1083.
13. P. H. GEIL, *ibid Vol. A2* (1964) 3813.
14. J. PETERMANN and H. GLEITER, *Phil. Mag.* **25** (1972) 813.
15. S. KAVESH and J. M. SCHULTZ, *Rev. Sci. Inst.* **40** (1969) 98.
16. J. PETERMANN and H. GLEITER, *Phil. Mag.* **31** (1975) 929.
17. "Mechanical Properties of Polymers" edited by N. M. Bikales (Wiley Interscience, New York, 1971) P. 28.

Received 10 January and accepted 6 May 1977.